HHS Public Access

Author manuscript

Am J Surg Pathol. Author manuscript; available in PMC 2021 June 10.

Published in final edited form as:

Am J Surg Pathol. 2019 April ; 43(4): 489–496. doi:10.1097/PAS.0000000000001200.

The *HTN3-MSANTD3* Fusion Gene Defines a Subset of Acinic Cell Carcinoma of the Salivary Gland

Simon Andreasen, MD, PhD[*,†,‡], **Sushama Varma, MS**[§], **Nicholas Barasch, MD**[‖], **Lester D.R. Thompson, MD**[¶], **Markku Miettinen, MD**[#], **Lisa Rooper, MD**[**], **Edward B. Stelow, MD**[††], **Tina K. Agander, MD, PhD**[‡], **Raja R. Seethala, MD**[‖], **Simion I. Chiosea, MD**[‖], **Preben Homøe, MD, PhD, DMSc**[†], **Irene Wessel, MD, PhD**[*], **Stine R. Larsen, MD**[‡‡], **Daiva Erentaite, MD**[§§], **Justin A. Bishop, MD**[‖‖], **Benedicte P. Ulhøi, MD**[¶¶], **Katalin Kiss, MD**[‡], **Linea C. Melchior, PhD**[‡], **Jonathan R. Pollack, MD, PhD**[§], **Robert B. West, MD, PhD**[§]

[*] Department of Otorhinolaryngology Head & Neck Surgery and Audiology, Rigshospitalet, Copenhagen University Hospital

[‡] Department of Pathology, Rigshospitalet, Copenhagen University Hospital, Copenhagen

[†] Department of Otorhinolaryngology and Maxillofacial Surgery, Zealand University Hospital, Køge

[‡‡] Department of Pathology, Odense University Hospital, Odense

[§§] Department of Pathology, Aalborg University Hospital, Aalborg

[¶¶] Department of Pathology, Aarhus University Hospital, Aarhus, Denmark

[§] Department of Pathology, Stanford University School of Medicine, Stanford, CA

[‖] Department of Pathology, University of Pittsburgh Medical Center, Pittsburgh, PA

[#] Laboratory of Pathology, NCI/NIH, Bethesda

[**] Department of Pathology, The Johns Hopkins Medical Institutions, Baltimore, MD

[¶] Southern California Permanente Medical Group, Woodland Hills, CA

[††] Department of Pathology, The University of Virginia, Charlottesville, VA

[‖‖] Department of Pathology, University of Texas Southwestern Medical Center, Dallas, TX

Abstract

The spectrum of tumors arising in the salivary glands is wide and has recently been shown to harbor a network of tumor-specific fusion genes. Acinic cell carcinoma (AciCC) is one of the more frequently encountered types of salivary gland carcinoma, but it has remained a genetic orphan until recently when a fusion between the *HTN3* and *MSANTD3* genes was described in one case. Neither of these 2 genes is known to be implicated in any other malignancy. This study was undertaken to investigate whether the *HTN3-MSANTD3* fusion is a recurrent genetic event in AciCC and whether it is a characteristic of one of its histological variants. Of the 273 AciCCs

Correspondence: Simon Andreasen, MD, PhD, Department of Otorhinolaryngology Head & Neck Surgery and Audiology, Rigshospitalet, Copenhagen University Hospital, Blegdamsvej 9, 2100 Copenhagen, Denmark, simon@andreasen.pm.

screened, 9 cases showed rearrangement of *MSANTD3* by break-apart fluorescence in situ hybridization, 2 had 1 to 2 extra signals, and 1 had gain, giving a total of 4.4% with *MSANTD3* aberrations. In 6 of 7 available cases with *MSANTD3* rearrangement, the *HTN3-MSANTD3* fusion transcript was demonstrated with real-time polymerase chain reaction. Histologically, all fusion-positive cases were predominantly composed of serous tumor cells growing in solid sheets, with serous tumor cells expressing DOG-1 and the intercalated duct-like cell component being CK7 positive and S-100 positive in 6/9 cases. All but one case arose in the parotid gland, and none of the patients experienced a recurrence during follow-up. In contrast, the case with *MSANTD3* gain metastasized to the cervical lymph nodes and lungs. In conclusion, we find the *HTN3-MSANTD3* gene fusion to be a recurrent event in AciCC with prominent serous differentiation and an indolent clinical course.

Keywords

carcinoma; acinic cell; salivary gland; salivary gland neoplasms; genes; HTN3-MSANTD3; gene fusion; genetics

Salivary gland acinic cell carcinoma (AciCC) constitutes ~10% of primary salivary gland carcinomas and arises in female individuals in two-thirds of cases.[1] Although typically a low-grade malignancy with a favorable long-term prognosis, the high-grade transformation is well described and is associated with an aggressive clinical course.[2,3] With the exception of frequent DOG-1 (ANO1) expression, the immunohistochemical profile of AciCC is nonspecific, and the diagnosis is based on the characteristic acinar differentiation, which is aided by demonstration of cytoplasmic PAS-positive zymogen granules, which are resistant to diastase digestion.[3,4] During the last decade, molecular studies have revealed numerous type-specific translocations in salivary gland tumors, which have become valuable diagnostic tools in equivocal cases and in cases of high-grade transformation, small biopsy specimens, so-called hybrid tumors, and even in fine-needle aspiration cytologies.[5–7]

In 2010, Skálová and colleagues separated a morphologically and genetically distinct subset of “zymogen granule-poor AciCC” from conventional AciCC, and they found this subset to be histologically and genetically identical to secretory carcinoma of the breast.[3,8–12] However, only recently was “classic” AciCC shown to belong to the group of salivary gland carcinomas driven by fusion oncogenes with the demonstration of a gene fusion between the Histatin 3 *(HTN3)* and Myb/SANT-like DNA-binding domain containing 3 *(MSANTD3)* genes in an index case, and rearrangement of *MSANTD3* in 2/19 additional AciCCs by fluorescence in situ hybridization (FISH).[13] Interestingly, rearrangement of the poorly characterized *MSANTD3* gene was found to be unique for AciCC among all other types of salivary gland tumors.[13] However, the *HTN3-MSANTD3* fusion was demonstrated in the index case only, and the prevalence of this novel gene fusion in AciCC has been uncertain due to the relatively small sample size in this initial report. Moreover, MSANTD3 expression was not sensitive or specific for AciCC.[13] Hence, the diagnostic, as well as prognostic, value of this gene fusion has remained unclarified.

In this study, we interrogated a large set of salivary gland AciCCs for the presence of *MSANTD3* rearrangement and characterized cases with aberrations for expression of the

HTN3-MSANTD3 fusion transcript. Moreover, we present the clinicopathologic data on the *MSANTD3*-rearranged AciCCs in order to ascertain the clinical course of this genetically distinct subset of AciCC.

MATERIALS AND METHODS

Patient Material

AciCC were retrieved from the surgical pathology archives from the authors' institutions, including the material previously included by Barasch et al.[13] Formalin-fixed paraffin-embedded (FFPE) blocks from 273 cases, including 5 cases with high-grade transformation, were retrieved and tissue microarrays constructed for the majority of cases after different protocols, either including large single cores or duplicate/triplicate 0.6 mm cores.[13,14] Whole slides were evaluated for the remaining cases. Clinical information was collected from patient files. The study was approved by the Danish Data Protection Agency (J.no. REG-94–2014) and the Ethics Committee of the Capital Region of Denmark (J.no. H-6–2014-086 add. 58080).

Histochemistry and Immunohistochemistry

From *MSANTD3*-rearranged cases and 20 nonrearranged controls, whole sections were cut to 4 μm slides and stained with hematoxylin and eosin (H&E), periodic acid-Schiff with (PAS+D) and without (PAS-D) diastase, phosphotungstic acid hematoxylin (PTAH), and Perls' prussian blue using standard protocols. Immunohistochemistry was performed as previously described using the antibodies listed in Table 1.[15,16] Briefly, sections were mounted on coated slides, deparaffinized using EZ-prep, and the antigens retrieved with CC1 in Tris buffer (pH 8.5) (all Ventana Medical Systems, Tucson, AZ). The ultraView DAB Detection kit (Ventana) was used for visualization, and slides were counterstained with Mayer's hematoxylin. Positive controls as suggested on datasheets were used on each slide, and the expected reaction and subcellular site were confirmed. Positive and negative controls were used on all slides.

Fluorescence In Situ Hybridization

In order to screen for *MSANTD3* rearrangement, the material was characterized using either a custom break-apart FISH probe for *MSANTD3* generated from bacterial artificial chromosomes flanking *MSANTD3,* CTD-3186I20 Cy5 (telomeric), and CTD-2363K7 Cy3 (centromeric) (BACPAC Resources Center, Children's Hospital Oakland Research Institute) labeled with either Cy5 or Cy3 (GE Healthcare Life Sciences, Chicago, IL) or a commercially available break-apart probe (Empire Genomics, Buffalo, NY), which was hybridized using Vysis (Abbott Molecular, Des Plaines, IL) reagents and protocols. After hybridization, nuclei were counterstained with DAPI II (ZytoVision, Bremerhaven, Germany), and the images were captured using Ariol software (Applied Imaging, San Jose, CA). For each case, 60 to 100 nuclei were evaluated and rearrangement defined as ≥ 1 split signal in ≥ 10% of nuclei.[8,17] The gain was defined as > 2 of one or both signals in ≥ 10% of nuclei.

Ribonuclease Acid Sequencing

Total ribonuclease acid (RNA) was prepared for RNA sequencing in accordance with the manufacturer's instructions (Illumina, San Diego, CA). RNA sequencing was performed using Illumina's TruSeq Stranded Total RNA Library Prep Kit, and paired-end sequencing was performed to gain an output of 100 M reads according to the manufacturer's instructions. FusionMap was used for the screening of fusion transcripts.[18]

Real-time Polymerase Chain Reaction and Nucleotide Sequence Analysis

Total RNA was isolated from FFPE sections using Maxwell RSC FFPE kit (Promega, Madison, WI) according to the manufacturer's instructions. RNA was converted to complementary deoxyribonucleic acid (cDNA) using the Superscript VILO cDNA synthesis kit (Thermo Fisher Scientific, Waltham, MA) and performed according to the manufacturer's instructions. RNA integrity was tested using primer pairs for the phosphoglycerate kinase gene (*PGK1*) in each case, as described previously.[19,20] The cDNA was subjected to real-time polymerase chain reaction (RT-PCR) using the primers TGAGACTTCACTTCAGCTTCAC (NM_000200) and CAACGAAATTATAAAGCCTGCCA (NM_080655) spanning the fusion site between exon 1 and exon 2 of *HTN3* and *MSANTD3,* respectively. PCR conditions were as follows: 94°C for 90 seconds followed by 40 cycles of 94°C for 45 seconds, 60°C for 1 minute, 72°C for 1 minute, and a final extension of 72°C for 10 minutes. T3 and T7 tails were attached to the forward and reverse primers, respectively, which were used for later sequencing of the amplified products. The amplified fusion products were visualized using Qiaxcel (Qiagen GmbH, Hilden, Germany), and the 160 bp amplicons were subsequently sequenced using BigDye Terminator 3.1 Cycle Sequencing Kit, T3/T7-primers, and an ABI 3500 Dx DNA sequenator according to the manufacturer's instructions (Thermo Fisher Scientific). Ten nonrearranged AciCCs were used as controls.

RESULTS

MSANTD3 Aberrations in AciCC

Among the 273 AciCCs comprising the cohort, 9 cases (3.3%) showed split signals with the *MSANTD3* probe in 17% to 48% percent of tumor cells, one case each showed 1 to 2 extra green and red signals, respectively, giving a total of 4% with *MSANTD3* aberrations (Table 2 and Fig. 1). In addition to the index case from the study by Barasch et al[13] (case 1, Table 2), RT-PCR identified the fusion between *HTN3* exon 1 and *MSANTD3* exon 2 in 6/7 rearranged cases with available tissue (lanes 1 to 6, Table 2, Fig. 2). Despite showing rearrangement of *MSANTD3* by FISH and having sufficient RNA quality for RT-PCR, no fusion transcript was identified in case 7, and RNA did not meet quality requirements for RNA sequencing. One case that showed a gain of one *MSANTD3* signal did not express a fusion transcript, which was also the case for 10 nonrearranged AciCCs (Fig. 3).

Clinical and Histologic Findings in AciCC With MSANTD3 Aberrations

The clinical and pathologic findings of the cases are summarized in Table 2. Sex was known in 10/11 cases with 3 male patients and 7 female patients, with ages ranging from 28 to 76

years (mean: 54 y). All except one arose in the parotid gland and varied in size from 12 to 110 mm in largest dimension (mean: 33 mm). Stage information was available for 6/11 patients, and all presented with localized disease. Treatment information was available for 9/11 patients, and all underwent surgical resection of the primary site and 3 received adjuvant radiotherapy. Follow-up was available for 6/11 patients and ranged from 24 to 269 months (median: 78 mo). None of the patients experienced a recurrence during follow-up, although case 10 itself was a recurrent tumor for which no additional information was available on the primary tumor. The case with *MSANTD3* gain arose in a 75-year-old woman who presented with cervical lymph node metastases and subsequently developed pulmonary metastases. She was lost to follow-up 3 months after pulmonary resection.

Only cores embedded in tissue microarrays were available in 4 cases, but the remaining cases ranged from well circumscribed (3/7) to locally invasive (4/7). All were lobulated lesions showing hallmark AciCC features with widespread to almost universally dominant neoplastic serous cells growing in solid sheets with pronounced cytoplasmic granulation (Figs. 3, 4A–D). Accordingly, the intercalated duct-like cell component was present in variable proportions ranging from minuscule to more conspicuous (Figs. 4C–F). Intercalated duct-like cells were variable in size and shape with eosinophilic to pale cytoplasm arranged in cysts, microcysts, and cribriform formations filled with a homogenous eosinophilic material (Figs. 4D–F). No areas of papillary or follicular growth or clear cell or oncocytic change were observed in any of the primary tumors, and none had lymphoid stroma or areas of high-grade transformation. Immunohistochemically, all available cases showed intense positivity for CK7 and S-100 in the intercalated duct-like component and intense expression of DOG-1 in the luminal membrane of serous tumor cells (Figs. 5A, B and Table 3). Alpha-amylase was expressed in the cytoplasmic granules of 6/10 cases (Fig. 5B, inset). Mammaglobin was consistently negative and Ki-67 index varied from 1% to 5% (mean: 2.2) (Table 3). This immunohistochemical profile was similar to what was found in 20 AciCCs without *MSANTD3* aberrations (Table 3).

DISCUSSION

The landscape of tumor-specific gene fusions in salivary gland tumors has grown increasingly complex during the last decade and was recently expanded to include AciCC with the description of the *HTN3-MSANTD3* fusion in one single case.[5,21–23] The *HTN3* gene encodes the histatin 3 peptide, which is secreted exclusively in saliva and has antimicrobial activity important in the maintenance of oral health.[24,25] As a consequence of the fusion, the highly active promoter region of *HTN3* is positioned to control the expression of the poorly characterized *MSANTD3* gene (Fig. 2B). Neither of these 2 genes has previously been reported to be recurrently involved in any type of malignancy, and aberrations in either of these genes are rare across the > 65,000 samples of various human malignancies listed in cBioPortal.[26] The oncogenic properties of the highly conserved *MSANTD3* are not well understood, but the gene shows some degree of homology with the *MYB* gene known from adenoid cystic carcinoma of the salivary gland and various other sites.[27–29] Furthermore, the oncogenic properties of *MSANTD3* are strongly supported by our finding of *MSANTD3* gain in one case with an unusually aggressive clinical course with marked local invasion and metastatic spread to cervical lymph nodes and lungs (Fig. 3). To

our knowledge, *MSANTD3* gain has not previously been reported in any type of malignancy.

We show the *HTN3* gene to be the partner gene in the majority of salivary gland AciCC with *MSANTD3* aberrations (Table 2). Considering the function of HTN3 in saliva, it is not unexpected that the *HTN3* gene is expressed exclusively in the serous acinar cell, and this cell, therefore, is the dominant one in *HTN3-MSANTD3*–driven tumors. Yet, although in a minor proportion, the intercalated duct-like cells were present in all cases, thereby suggesting an ability of the serous cell to differentiate into this particular cell type. However, the one case arising outside the parotid gland (case 8) did not harbor this fusion transcript by RT-PCR, and RNA sequencing failed to be informative about the fusion status of this particular case due to insufficient RNA quality. Hence, we can only speculate whether the fusion partner, in this case, was fused to a different exon of *HTN3* or an entirely different gene, most likely a gene with a highly active promoter region.

In our expanded material of 273 cases, including the material from Barasch et al,[13] we found *MSANTD3* aberrations in a low proportion of AciCCs (4.4%), as compared with the 15% originally reported (Table 2). The histologic hallmark of AciCC is the serous cell component, which is present in variable proportions, together with the intercalated duct-like component growing in one or more different patterns, which include solid, microcystic, papillary-cystic, and follicular. Interestingly, with the exception of the case with isolated *MSANTD3* gain, the AciCCs with *MSANTD3* aberrations were all highly differentiated "classic" AciCCs dominated by serous tumor cells in a solid growth pattern. Moreover, none of the cases had significant lymphoid infiltrates, an otherwise common finding in AciCC and associated with a favorable outcome.[30]

We found an identical immunohistochemical profile between our 12 cases and wild-type controls, distinctly different from that of secretory carcinoma, which was recently separated from AciCC (Table 3).[8,31] Therefore, the archetypical features of AciCC with *MSANTD3* rearrangement is solid growth, serous cell domination, and absence of lymphoid stroma. However, these characteristics are not unique to AciCC with *MSANTD3* aberrations, and the clinical impact of identifying these patients is unlikely to be of significance, as the clinical course of the present material did not differ from the generally indolent nature of AciCC. Collectively, these findings do not merit the separation of *MSANTD3*-rearranged AciCC as a diagnostic entity, but rather as a genetic characteristic of a subset of classic AciCC.

Similarities between tumors of the salivary gland and breast are well known and include several entities in which identical fusion genes are found in histologically identical tumors of both sites, including adenoid cystic carcinoma and secretory carcinoma.[29,32] Among the most intensely debated of these is breast AciCC, as it has a genetic profile similar to other triple-negative breast carcinomas with a high proportion of *TP53* mutations, whereas the mutational burden in salivary AciCC is low.[32–35] However, in contrast to most triple-negative breast carcinomas, AciCC has a favorable prognosis similar to other salivary-type breast carcinomas found in the breast.[32] The identification of a gene fusion involving the

promoter region of the *HTN3* gene, a gene not expressed in the breast, lends further support to AciCC of the salivary gland and that of the breast as being distinctly different entities.[24]

In conclusion, the *HTN3-MSANTD3* fusion is a recurrent fusion event in the salivary gland AciCC but is found in <5% of cases, in particular, those dominated by serous tumor cells in a solid growth pattern without lymphoid stroma. Although we report on relatively few cases of which one case with *MSANTD3* gain metastasized, the clinical course of patients with *MSANTD3* aberrations is not distinct from that of AciCC in general. The molecular underpinnings for the vast majority of AciCC remain unknown and await further investigation.

ACKNOWLEDGMENT

The authors express their gratitude to Camilla Cordua Mortensen for invaluable assistance with RT-PCR

Conflicts of Interest and Source of Funding: The authors have disclosed that they have no significant relationships with, or financial interest in, any commercial companies pertaining to this article.

REFERENCES

1. Bjø rndal K, Krogdahl A, Therkildsen MH, et al. Salivary gland carcinoma in Denmark 1990–2005: a national study of incidence, site and histology. Results of the Danish Head and Neck Cancer Group (DAHANCA). Oral Oncol. 2011;47:677–682. [PubMed: 21612974]
2. Thompson LD, Aslam MN, Stall JN, et al. Clinicopathologic and immunophenotypic characterization of 25 cases of acinic cell carcinoma with high-grade transformation. Head Neck Pathol. 2016;10:152–160. [PubMed: 26245749]
3. Chiosea SI, Griffith C, Assaad A, et al. The profile of acinic cell carcinoma after recognition of mammary analog secretory carcinoma. Am J Surg Pathol. 2012;36:343–350. [PubMed: 22301503]
4. Wenig BM. Neoplasms of the salivary glands. In: Wenig BM, ed. Atlas of Head and Neck Pathology, 3rd ed. Philadelphia, PA: Elsevier; 2015:499–504.
5. Andersson MK, Stenman G. The landscape of gene fusions and somatic mutations in salivary gland neoplasms—implications for diagnosis and therapy. Oral Oncol. 2016;57:63–69. [PubMed: 27101980]
6. Hudson JB, Collins BT. MYB gene abnormalities t(6;9) in adenoid cystic carcinoma fine-needle aspiration biopsy using fluorescence in situ hybridization. Arch Pathol Lab Med. 2014;138:403–409. [PubMed: 24576033]
7. Bishop J, Westra W. MYB translocation status in salivary gland epithelial-myoepithelial carcinoma: evaluation of classic, variant, and hybrid forms. Am J Surg Pathol. 2017;42:319–325.
8. Skálová A, Vanecek T, Sima R, et al. Mammary analogue secretory carcinoma of salivary glands, containing the ETV6-NTRK3 fusion gene: a hitherto undescribed salivary gland tumor entity. Am J Surg Pathol. 2010;34:599–608. [PubMed: 20410810]
9. Skálová A, Bell D, Bishop J, et al. Secretory carcinoma. In: El-Naggar A, Chan J, Grandis J, Takata T, Slootweg P, eds WHO Classification of Head and Neck Tumours, 4th ed. Lyon: IARC Press; 2017: 177–178.
10. Bishop JA. Unmasking MASC: bringing to light the unique morphologic, immunohistochemical and genetic features of the newly recognized mammary analogue secretory carcinoma of salivary glands. Head Neck Pathol. 2013;7:35–39. [PubMed: 23459839]
11. Chiosea SI, Peel R, Barnes EL, et al. Salivary type tumors seen in consultation. Virchows Arch. 2009;454:457–466. [PubMed: 19271235]
12. Griffith C, Seethala R, Chiosea SI. Mammary analogue secretory carcinoma: a new twist to the diagnostic dilemma of zymogen granule poor acinic cell carcinoma. Virchows Arch. 2011;459:117–118. [PubMed: 21638010]

13. Barasch N, Gong X, Kwei KA, et al. Recurrent rearrangements of the Myb/SANT-like DNA-binding domain containing 3 gene (MSANTD3) in salivary gland acinic cell carcinoma. PLoS One. 2017;12:e0171265. [PubMed: 28212443]
14. Miettinen M A simple method for generating multitissue blocks without special equipment. Appl Immunohistochem Mol Morphol. 2012;20:410–412. [PubMed: 22495380]
15. Andreasen S, Therkildsen MH, Grauslund M, et al. Activation of the interleukin-6/Janus kinase/STAT3 pathway in pleomorphic adenoma of the parotid gland. APMIS. 2015;123:706–715. [PubMed: 26061266]
16. Andreasen S, Persson M, Kiss K, et al. Genomic profiling of a rare case of combined large-cell neuroendocrine carcinoma of the submandibular gland. Oncol Rep. 2016;35:2177–2182. [PubMed: 26883388]
17. Andreasen S, Bishop JA, Hansen TV, et al. Human papillomavirus-related carcinoma with adenoid cystic-like features of the sinonasal tract: clinical and morphological characterization of 6 new cases. Histopathology. 2016;70:880–888.
18. Ge H, Liu K, Juan T, et al. FusionMap: detecting fusion genes from next-generation sequencing data at base-pair resolution. Bioinformatics. 2011;27:1922–1928. [PubMed: 21593131]
19. Argani P, Perez-Ordonez B, Xiao H, et al. Olfactory neuroblastoma is not related to the Ewing family of tumors: absence of EWS/FLI1 gene fusion and MIC2 expression. Am J Surg Pathol. 1998;22: 391–398. [PubMed: 9580174]
20. Andreasen S, Skálová A, Agaimy A, et al. ETV6 gene rearrangements characterize a morphologically distinct subset of sinonasal low-grade non-intestinal-type adenocarcinoma: a novel translocation-associated carcinoma restricted to the sinonasal tract. Am J Surg Pathol. 2017;41:1552–1560. [PubMed: 28719468]
21. Weinreb I, Piscuoglio S, Martelotto LG, et al. Hotspot activating PRKD1 somatic mutations in polymorphous low-grade adenocarcinomas of the salivary glands. Nat Genet. 2014;46:1166–1169. [PubMed: 25240283]
22. Kawahara A, Harada H, Abe H, et al. Nuclear β-catenin expression in basal cell adenomas of salivary gland. J Oral Pathol Med. 2011;40:460–466. [PubMed: 21323741]
23. Chiosea SI, Miller M, Sethala RR. HRAS mutations in epithelial-myoepithelial carcinoma. Head Neck Pathol. 2014;8:146–150. [PubMed: 24277618]
24. Uhlén M, Fagerberg L, Hallström BM, et al. Proteomics: tissue-based map of the human proteome. Science. 2015;347:1260419. [PubMed: 25613900]
25. Khurshid Z, Najeeb S, Mali M, et al. Histatin peptides: pharmacological functions and their applications in dentistry. Saudi Pharm J. 2017;25:25–31. [PubMed: 28223859]
26. Cerami E, Gao J, Dogrusoz U, et al. The cBio Cancer Genomics Portal: an open platform for exploring multidimensional cancer genomics data. Cancer Discov. 2012;2:401–404. [PubMed: 22588877]
27. Persson M, Andrén Y, Mark J, et al. Recurrent fusion of MYB and NFIB transcription factor genes in carcinomas of the breast and head and neck. Proc Natl Acad Sci USA. 2009;106:18740–18744. [PubMed: 19841262]
28. Brill LB II, Kanner WA, Fehr A, et al. Analysis of MYB expression and MYB-NFIB gene fusions in adenoid cystic carcinoma and other salivary neoplasms. Mod Pathol. 2011;24:1169–1176. [PubMed: 21572406]
29. Andreasen S, Tan Q, Agander TK, et al. Adenoid cystic carcinomas of the salivary gland, lacrimal gland, and breast are morphologically and genetically similar but have distinct microRNA expression profiles. Mod Pathol. 2018;31:1211–1225. [PubMed: 29467480]
30. Michal M, Skalová A, Simpson RH, et al. Well-differentiated acinic cell carcinoma of salivary glands associated with lymphoid stroma. Hum Pathol. 1997;28:595–600. [PubMed: 9158708]
31. Bishop JA, Yonescu R, Batista D, et al. Utility of mammaglobin immunohistochemistry as a proxy marker for the ETV6-NTRK3 translocation in the diagnosis of salivary mammary analogue secretory carcinoma. Hum Pathol. 2013;44:1982–1988. [PubMed: 23773480]
32. Geyer FC, Pareja F, Weigelt B, et al. The spectrum of triple-negative breast disease. Am J Pathol. 2017;187:2139–2151. [PubMed: 28736315]

33. Piscuoglio S, Hodi Z, Katabi N, et al. Are acinic cell carcinomas of the breast and salivary glands distinct diseases? Histopathology. 2015;67:529–537. [PubMed: 25688711]

34. Guerini-Rocco E, Hodi Z, Piscuoglio S, et al. The repertoire of somatic genetic alterations of acinic cell carcinomas of the breast: an exploratory, hypothesis-generating study. J Pathol. 2015;237:166–178. [PubMed: 26011570]

35. Grünewald I, Vollbrecht C, Meinrath J, et al. Targeted next generation sequencing of parotid gland cancer uncovers genetic heterogeneity. Oncotarget. 2015;6:18224–182237. [PubMed: 26053092]

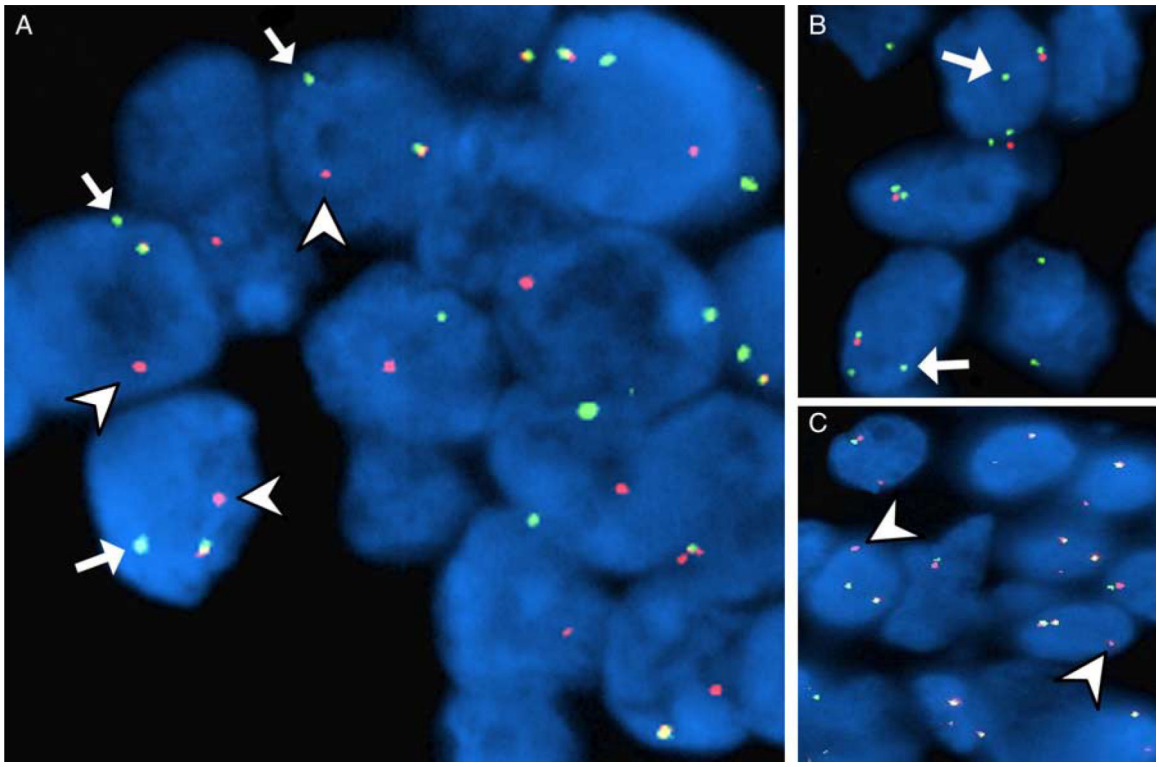

FIGURE 1.

Patterns of *MSANTD3* aberrations in acinic cell carcinoma of the salivary gland. A, FISH demonstrating separate green (arrows) and red (arrowheads) signals, consistent with fusion gene formation. The gain of one green signal (arrows) (B) and one red signal (arrowheads) (C) was present in a subset of cases.

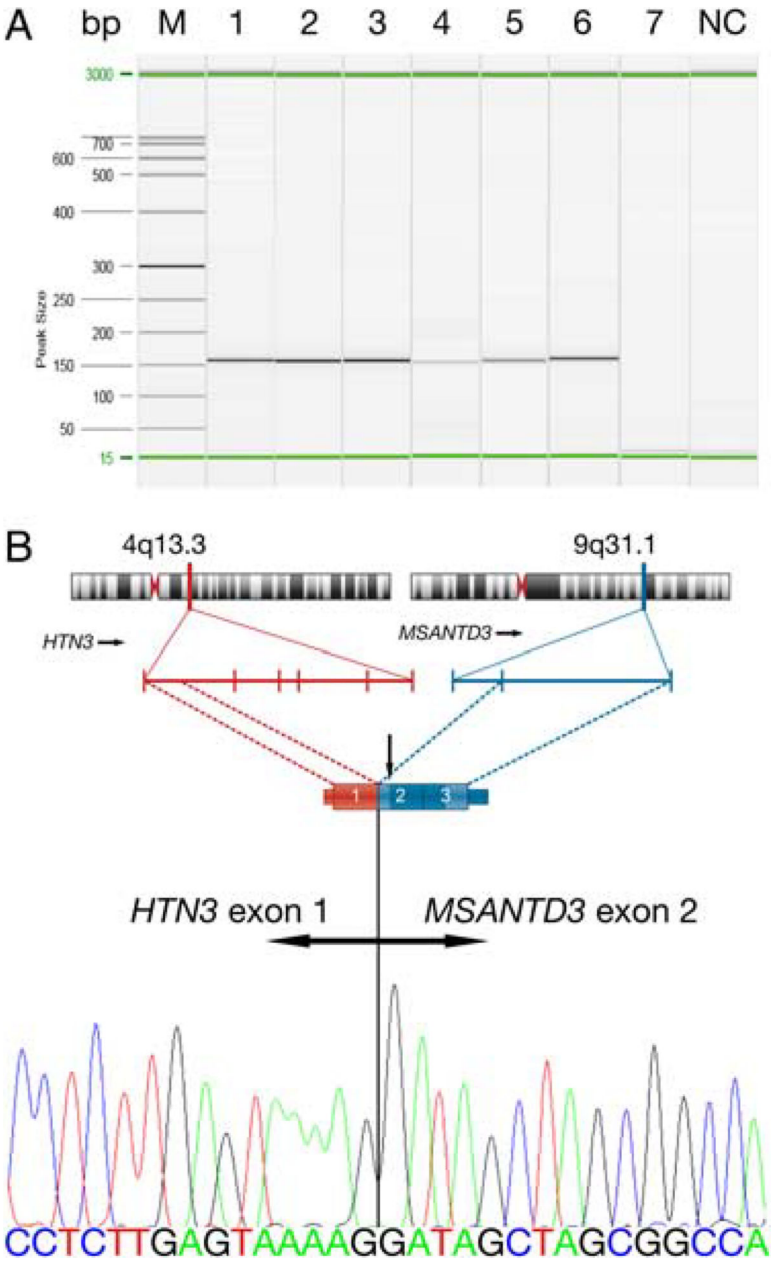

FIGURE 2. HTN3-MSANTD3

HTN3-MSANTD3 fusion transcripts in acinic cell carcinoma of the salivary gland. A, RT-PCR revealed a 160 bp fragment in cases 1 to 6 but not in case 7. RT-PCR did not yield an amplicon in any of the cases with complex *MSANTD3* FISH patterns (not shown). All cases had *PGK1* products, ensuring sufficient RNA quality (not shown). B, The breakpoints within the genomic location of the *HTN3* gene on chromosome 4 and *MSANTD3* gene on chromosome 9 with exons denoted by vertical bars schematically presented. An illustrative part of the fusion transcript demonstrating the fusion of exon 1 of *HTN3* and exon 2 of *MSANTD3*, which was shown to be the same in all 6 cases with amplified PCR fragments by nucleotide sequencing. Note that the start codon (vertical arrow) lies within exon 2 of

MSANTD3, causing for full-length MSANTD3 transcripts as marked by dark blue. Bp indicates base pair; M, marker; NC, negative control.

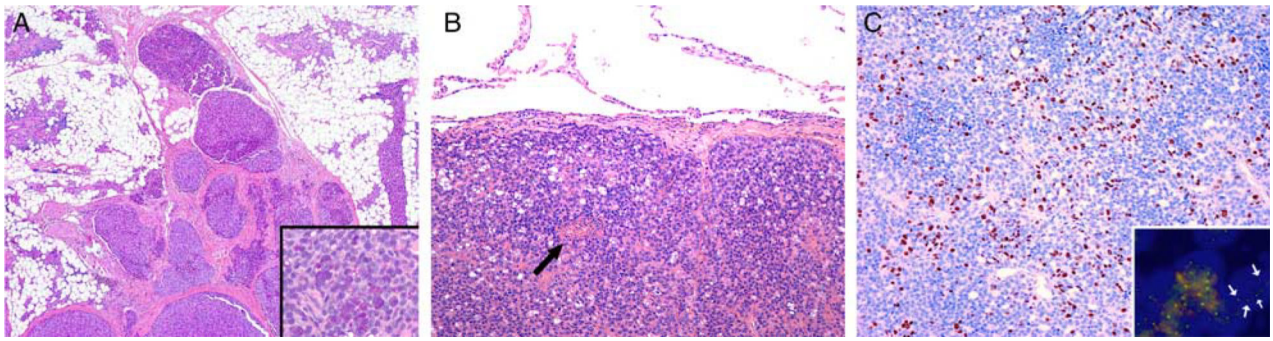

FIGURE 3.

Invasive growth of salivary gland acinic cell carcinoma with MSANTD3 gain. A, A locally invasive tumor growing along interlobular fibrous septae in an atrophic parotid gland (H&E). Note the preservation of cytoplasmic PAS+D-positive granulation (inset). B, A microcystic pulmonary metastasis from the tumor shown in (A) surrounded by a pseudocapsule with a small necrotic area (arrow, H&E). C, The proliferative activity as ascertained with Ki-67 was 10%, up to 25% in hotspots (Ki-67, IHC). The gain of the green signal in *MSANTD3* was found in the primary tumor as well as the metastasis (inset, arrows).

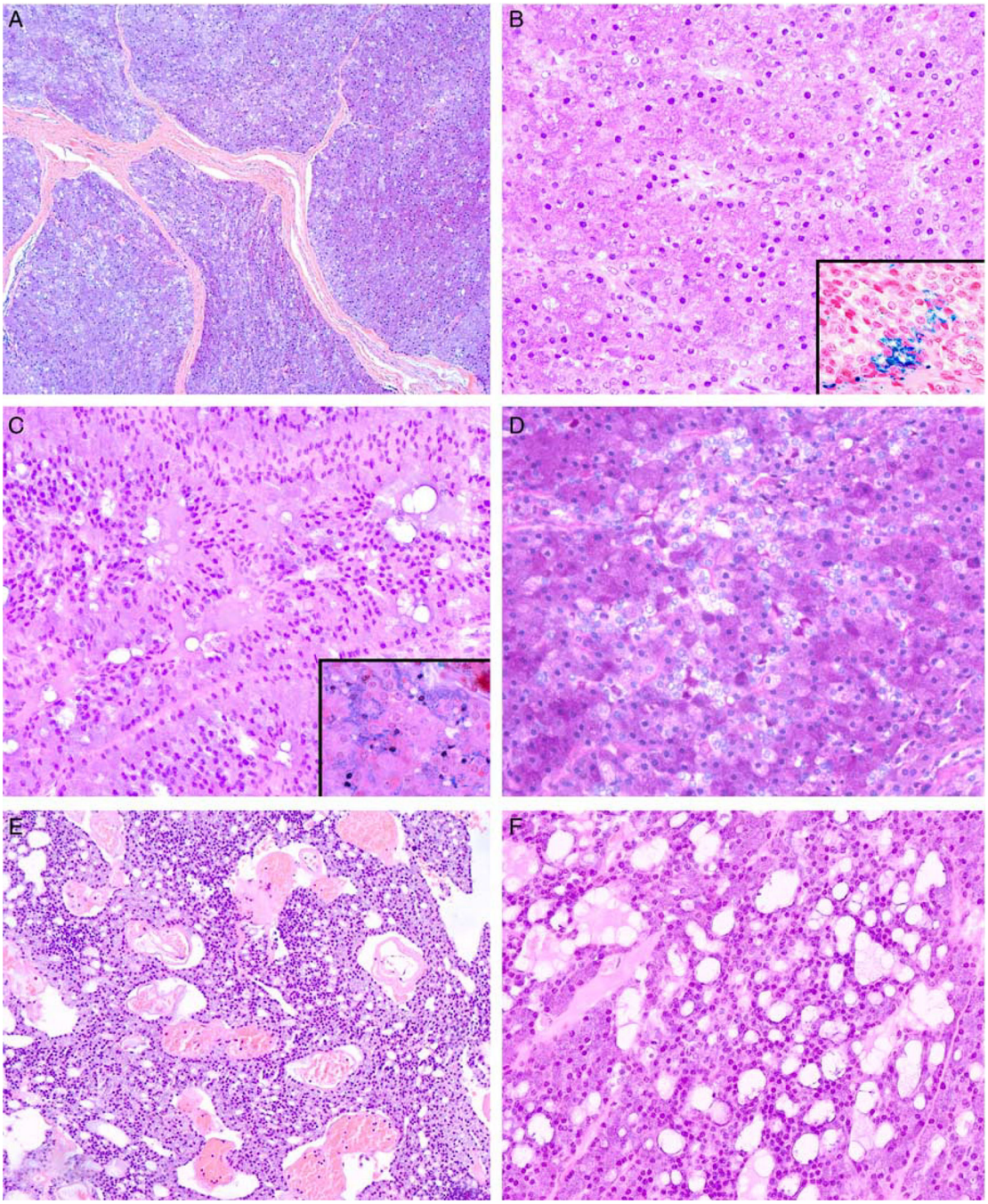

FIGURE 4.

Histologic spectrum of salivary gland acinic cell carcinoma with *MSANTD3* aberrations. A, Low-power magnification of a lobulated lesion composed of serous tumor cells in a solid growth pattern (H&E). B, High-power magnification of this cellular lesion showing these serous tumor cells with poorly defined borders, membrane-bound nuclei, and minimal intervening stroma (H&E). Minute cytoplasmic vacuoles are widespread, and hemosiderin granules are only rarely encountered (inset). C, Tumor cells showed occasional remnants of acinar arrangements and discrete cytoplasmic granulation readily discernable with PTAH

(inset). Intercalated duct-like tumor cells line small luminae with eosinophilic secretion. Note the basally located nuclei in tumor cells growing along thin fibrovascular septae (H&E). D, Cytoplasmic granulation was present in all cases to a variable extent but was pronounced in most cases. The intercalated duct-like cell component had eosinophilic to pale cytoplasm, as exemplified by the central portion of this image (H&E). E, Low-power view showing larger cysts and cribriform growth mainly lined by intercalated duct-like cells with interspersed neoplastic serous cells (H&E). F, Most cases had areas of microcystic overgrowth with evenly distributed serous and intercalated duct-like tumor cells. Microcysts were filled with variable amounts of bubbly eosinophilic secretion (H&E).

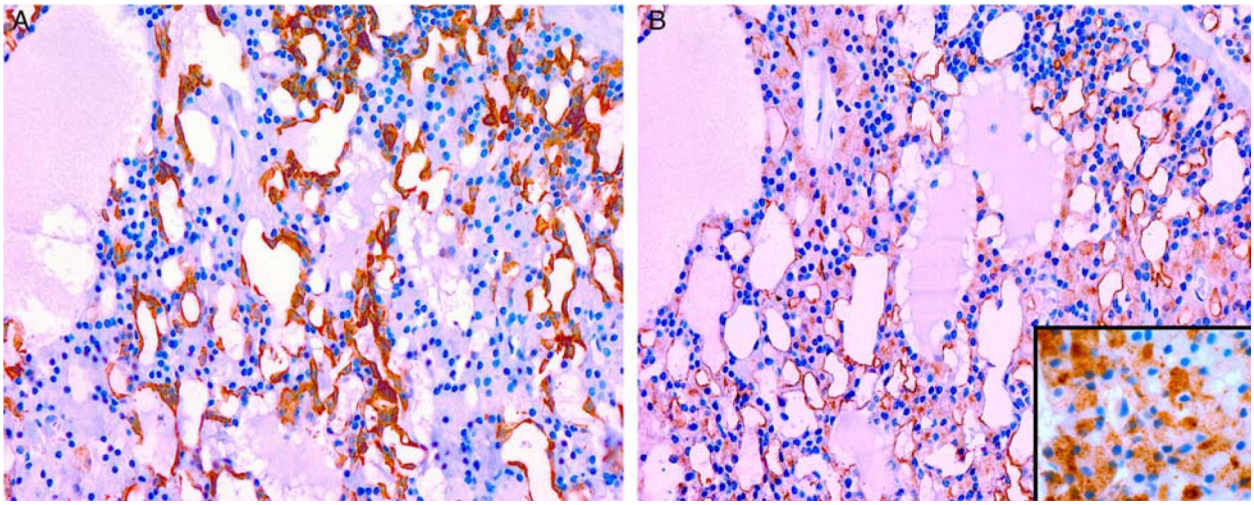

FIGURE 5.

Immunohistochemical profile of salivary gland acinic cell carcinoma with *MSANTD3* aberrations. A, S-100 highlights the cytoplasm of intercalated duct-like cells with serous cells being negative. B, DOG-1 highlight the luminal membrane of serous tumor cells with only a few, scattered intercalated duct-like cells showing faint cytoplasmic staining. Alpha-amylase highlights the cytoplasmic granules of the serous tumor cells (inset).

TABLE 1.

Antibodies Used for Immunohistochemical Characterization

Antibody	Clone	Dilution	Source
Alpha-amylase	EPR19605	1:10,000	AbCam (Cambridge, UK)
CK7	OV-TL 12/30	1:1000	Dako (Glostrup, Denmark)
DOG-1	SP31	Ready-to-use	Roche (Hvidovre, Denmark)
Ki-67	MIB1	1:100	Dako
Mammaglobin	304–1A5	Ready-to-use	Dako
S-100	Polyclonal	1:4,000	Dako

TABLE 2.

Demographics, Presentation, Treatment, and Outcome of Patients With *MSANTD3* Aberrated Acinic Cell Carcinoma

Case#	*MSANTD3* FISH	RT-PCR	Age (y), Sex	Site	Size (mm)	Presentation	Stage	Treatment	Outcome, follow-up (mo)
1	Break	*HTN3-MSANTD3*	59, M	Parotid	30×35×30	Parotid mass	T2N0M0	Surgery	DOC 98
2	Break	*HTN3-MSANTD3*	52, F	Parotid	80×110	Parotid mass	T3N0M0	Surgery+RT	NED 269
3	Break	*HTN3-MSANTD3*	51, F	Parotid	NA	NA	NA	NA	NA
4	Break	*HTN3-MSANTD3*	75, F	Parotid	25	Parotid mass	T2cN0M0	Surgery+RT	NED 120
5	Break	*HTN3-MSANTD3*	65, F	Parotid, accesssory	18	Buccal mass	T1cN0M0	Surgery	NED 36
6	Break	*HTN3-MSANTD3*	28, F	Parotid	32	Incidental finding on MRI	T2cN0M0	Surgery	NED 24
7	Break	—*	59, M	Submandibular	25×20×25	Submandibular mass	T2N0M0	Surgery+RT	NED 58
8†	Break	*HTN3-MSANTD3*‡	76, F	Parotid	25	NA	NA	Surgery	NA
9†	Break	NA	49, F	Parotid	12	NA	NA	Surgery	NA
10†	Break	NA	30, M	Parotid	12 (recurrence)	NA	NA	Surgery	NA
11	Break	NA	NA	Parotid	NA	NA	NA	NA	NA

*Absence of *HTN3-MSANTD3* fusion transcript by RT-PCR and uninformative RNA sequencing.

†Cases previously reported by Barasch et al[13] "Complex pattern, 1 to 2 extra green signals." "Complex pattern, 1 to 2 extra red signals."

‡Fusion identified by RNA sequencing.

DOC indicates died of other causes; MRI, magnetic resonance imaging; NA, not available; NED, no evidence of disease; RT, radiotherapy.

TABLE 3.

Immunohistochemical Profile of Acinic Cell Carcinoma With and Without *MSANTD3* Aberrations

Case#	Alpha amylase	CK7	DOG-1	Ki-67	Mammaglobin	S-100
1	+	+	+	2%	−	+
2	+	+	+	1%	−	+
3	NA	NA	+	NA	NA	NA
4	+	+	+	2%	−	−
5	−	+	+	1%	−	−
6	−	+	+	2%	−	−
7	−	+	+	4%	−	+
8	+	+	+	1%	−	+
9	−	+	+	2%	−	+
10	+	+	+	5%	−	+
Total	6/9	9/9	10/10	Mean 2.2	0/9	6/9
Non-rearranged AciCC (n = 20)	11/20	20/20	20/20	Mean 2	0/20	20/20

No material from case 11 was available for immunohistochemistry.

NA indicates not available.